Table 3 Predictor of blood platelet count after splenectomy by multiple logistic regression analysis in 55 patients with splenectomy

	OR (95% CI)	*P*-value
Blood red cell count before splenectomy (≧380 /μl)	2.41 (0.75–8.52)	0.14
ALT level before splenectomy (<38 IU/l)	3.4 (0.96–13.44)	0.05
PT level before splenectomy (<75%)	2.7 (0.83–9.53)	0.1

ALT serum alanine aminotransferase level; *CI* confidence interval, *OR* odds ratio, *PT* prothrombin percentage activity

Multiple logistic regression analysis was performed to identify which variables were independently associated with the blood platelet count 3 months after splenectomy (Table 3). Preoperative serum ALT level was independent predictors of the blood platelet count 3 months after splenectomy (<38 IU/l, OR 3.4, 95% CI 0.96–13.44, $P = 0.05$).

Blood platelet count and serum ALT level

Among 55 patients, 40 patients had high serum ALT level (≧38 IU/l). In both patients with high ALT level and low ALT level, blood platelet count significantly improved 3 months after splenectomy (low serum ALT patients, $n = 15$, from $4.2 \pm 1.3 \times 10^4/mm^3$ to $21.2 \pm 10 \times 10^4/mm^3$, $P < 0.01$; Fig. 1a) (high serum ALT patients, $n = 40$, from $4.5 \pm 1.6 \times 10^4/mm^3$ to $16 \pm 6 \times 10^4/mm^3$, $P < 0.01$; Fig. 1b). Three months after splenectomy, blood platelet count of patients with high serum ALT level were significantly lower than those of patients with low serum ALT level ($P = 0.02$) (Fig. 1c). In 55 cirrhotic patients who underwent splenectomy, blood platelet count 3 months after splenectomy decreased along with an increase in preoperative serum ALT level ($r = 0.67$, $P = 0.03$) (Fig. 1d).

Pathological findings of liver tissues

In nine patients who underwent hepatectomy and splenectomy on one stage surgery, all non-cancerous liver tissues showed bridging fibrosis with diffuse lobar distortion (stage 4) (Fig. 2a). In patients with liver cirrhosis, platelets were present predominantly in the sinusoids of the periportal area with inflammation. In cirrhotic patients with high serum ALT level, platelets were observed along the destructed limiting plate of the expanded fibrous portal area with inflammation and in the sinusoids of the periportal area (Fig. 2b,c). In all liver tissues including normal controls and nine cirrhotic patients who underwent hepatectomy and splenectomy on one stage surgery, there were platelets but no megakaryocytes in the sinusoids. Liver tissues of patients with high serum ALT level showed a significantly higher degree of inflammation than those of patients with low serum ALT level (grade; 2 ± 1 vs. 1 ± 1, $P = 0.03$) (Fig. 3a). In control liver tissues, there were a few lymphocytes, but only in the portal area, and neither necroinflammatory reactions nor fibrosis were noted (grade 0, stage 0).

Morphometry revealed that patients with cirrhosis had more extensive platelet area in the liver tissues than controls. In nine cirrhotic patients who underwent hepatectomy and splenectomy, the platelet area in liver tissues increased along with an increase in a grade of hepatic inflammation ($r = 0.86$, $P = 0.02$) (Fig. 3b). Blood platelet count 3 months after splenectomy was negatively correlated with platelet area of the liver tissues by Pearson correlation calculations ($r = 0.49$, $P = 0.03$) (Fig. 3c). There was no significant correlation between platelet area of the liver tissues and blood platelet count before splenectomy ($r = 0.01$, $P = 0.83$) (Fig. 3d). In patients with liver cirrhosis, the platelet area in liver tissues of patients with high serum ALT level were larger than those of patients with low serum ALT level ($18\,233 \pm 11\,188\ \mu m^2$ vs. $6672 \pm 5257\ \mu m^2$, $P = 0.14$).

Pathological findings of splenic tissues

In all splenic tissues, including cirrhotic patients with high or low serum ALT level and normal controls, platelets were diffusely found in the splenic sinus and splenic cord of the red pulp (Fig. 4a,b). Among the splenic tissues of nine cirrhotic patients who underwent hepatectomy and splenectomy on one stage surgery, megakaryocytes were observed in those of six patients (67%). CD41-positive-megakaryocytes were present in the splenic cord of the red pulp (Fig. 4c). There were no megakaryocytes in normal control tissues. Platelet area in splenic tissues of cirrhotic patients with high serum ALT level and those of patients with normal serum ALT level were $47\,685 \pm 22\,806\ \mu m^2$ and $78\,550 \pm 6550\ \mu m^2$, respectively.

Discussion

The exact mechanisms leading to thrombocytopenia in liver cirrhosis and the platelet kinetics of patients with chronic liver disease or cirrhosis are not well characterized. In this study, we demonstrated the histopathological findings of platelets in human hepatosplenic tissue and investigated the interaction between blood platelets and platelets of hepatosplenic tissues in cirrhotic patients.

Splenectomy [8, 9] and partial splenic arterial embolization [10] are therapies for thrombocytopenia caused by hypersplenism. Platelet kinetic studies using platelet scintigraphy have been reported [1, 2, 14–16].

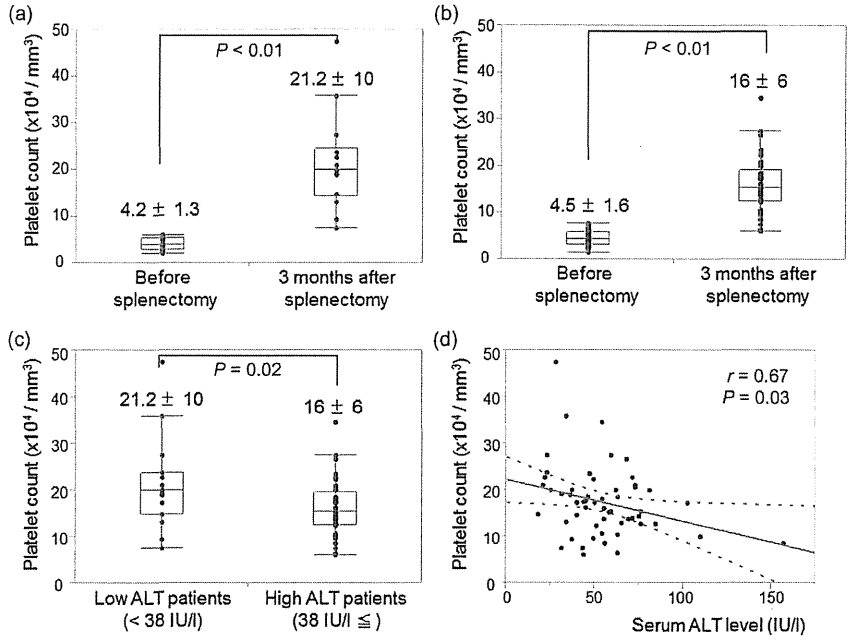

Fig. 1 Relationship between serum alanine aminotransferase (ALT) level and blood platelet count in 55 patients with splenectomy. (**a**) In 15 patients with low ALT level, comparison of the blood platelet count between before splenectomy and 3 months after. (**b**) In 40 patients with high ALT level, comparison of the blood platelet count between before splenectomy and 3 months after. (**c**) Three months after splenectomy, comparison of the blood platelet count between patients with high and low serum ALT level. (**d**) Correlation with the preoperative serum ALT level and the blood platelet count 3 months after splenectomy

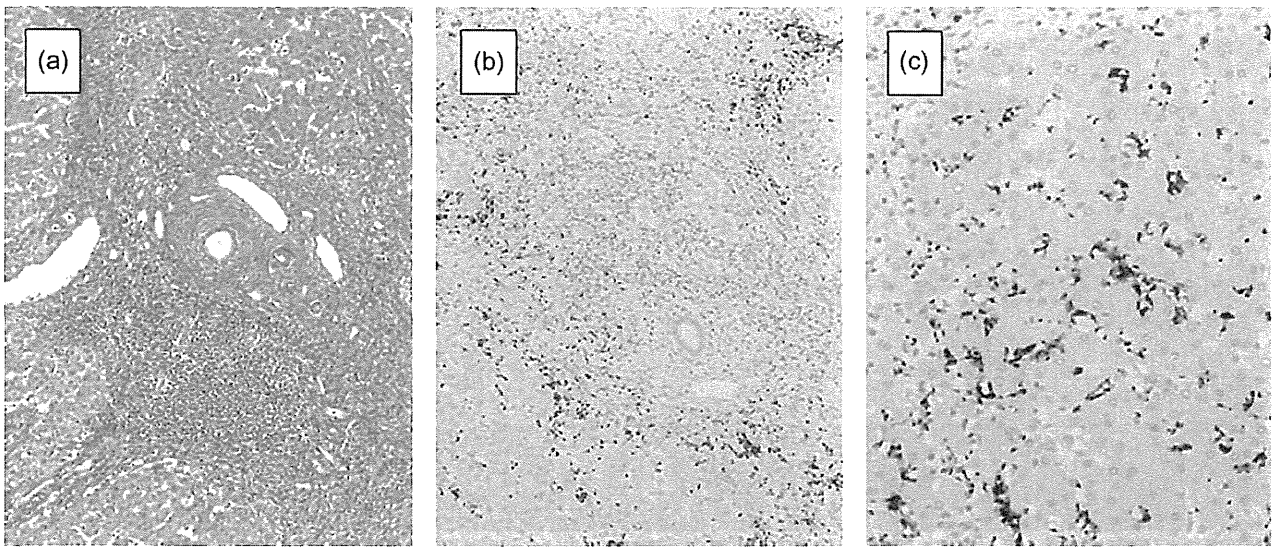

Fig. 2 Pathological findings of the liver tissues. (**a**) In liver tissue of cirrhotic patient with high serum alanine aminotransferase (ALT) level, there are strong inflammatory reactions in the portal area and destroyed limiting plate. Serum ALT 89 IU/l, grade 3, stage 4, stained with hematoxylin and eosin, × 100. (**b**) In liver tissue of cirrhotic patient with high serum ALT level, strong CD41 positive reactions are observed predominantly along the destroyed limiting plate of the expanded fibrous portal area with inflammation and in the sinusoidal space of the periportal area. Serum ALT 89 IU/l, grade 3, stage 4, immunostained with antibody against CD41, × 100. (**c**) Close up view of **b**. immunostained with antibody against CD41, × 200

Noguchi et al. [14] reported that partial splenic arterial embolization induced an increase in the blood platelet count and a decrease in the spleen/liver uptake ratio of ^{111}In-labeled platelets. In patients with thrombocytopenia, Kinuya et al. [15] reported that the spleen/liver uptake ratio for ^{111}In- or ^{99}Tc-labeled platelets was apparently lower in patients for whom splenectomy was ineffective than in those for whom it was effective. Based on these previous reports, splenectomy and partial splenic arterial embolization induce a decrease in platelet pooling or breakdown in the spleen of thrombocytopenic patients, and, as a result, the blood platelet count increased.

In this study, we found that blood platelet counts of cirrhotic patients with high serum ALT levels tended to only slightly improve after splenectomy. In a recent study, we reported that the accumulation of platelets in the liver with

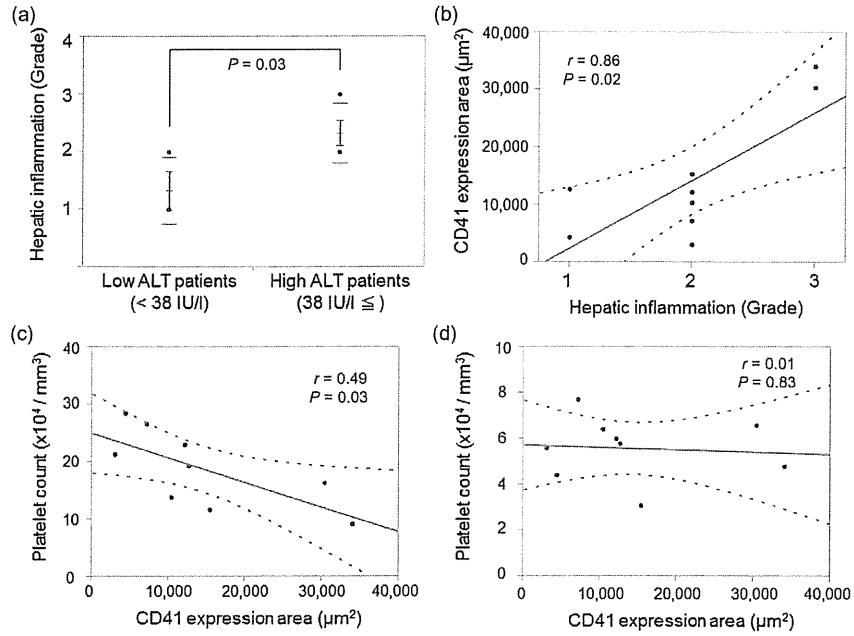

Fig. 3 Relationship between serum alanine aminotransferase (ALT) level, histologic inflammatory activity of liver tissues, and blood platelet count. (**a**) Comparison of the histologic inflammatory activity of liver tissues between patients with high and low serum ALT level. (**b**) Correlation with the platelet area of liver tissues and the histologic inflammatory activity of liver tissues. (**c**) Correlation with platelet area of liver tissues and the blood platelet count 3 months after splenectomy. (**d**) Correlation with platelet area of liver tissues and the blood platelet count before splenectomy

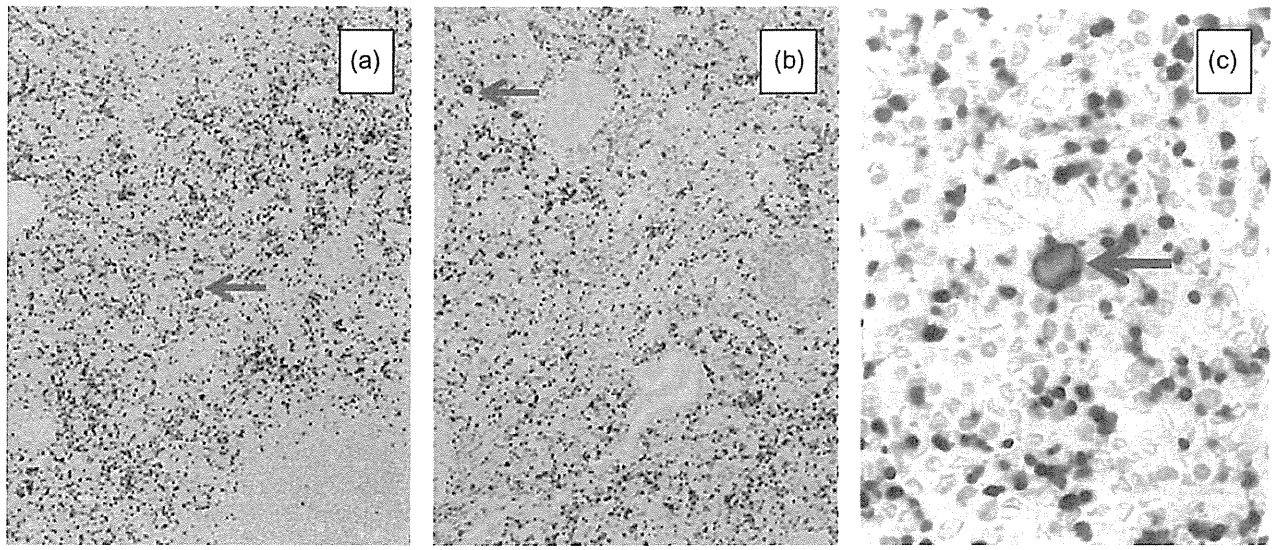

Fig. 4 Pathological findings of splenic tissues. (**a, b**) In the splenic tissue of cirrhotic patient with low (**a**) or high (**b**) serum alanine aminotransferase (ALT) level, CD41 positive reactions are diffusely observed in the splenic sinus and splenic cord of the red pulp. Megakaryocyte (arrow) is encountered in the splenic cord. immunostained with antibody against CD41, × 40; (**a**) Serum ALT 8 IU/l, grade 1, stage 4; (**b**) Serum ALT 89 IU/l, grade 3, stage 4. (**c**) Close up view of **b**. immunostained with antibody against CD41, × 200

chronic hepatitis and cirrhosis is one of the important contributory factors to thrombocytopenia [7]. The accumulation of platelets in noncancerous liver tissues of patients with chronic hepatitis or cirrhosis increased with an increase in the histological liver damage [7]. Platelets may accumulate in the sinusoids under thrombocytotic conditions in chronic hepatitis brought about by the activated hepatic reticuloendothelial system, as caused by inflammation [7, 17–20].

In blood vessels, the vessel wall, with its inner lining of endothelium, is crucial to the maintenance of a patent vasculature. The endothelium contains thromboregulators, nitric oxide, prostacyclin, and the ectonucleotidase CD39, which together provide a defense against platelet thrombus formation [21]. When the endothelium is disrupted, collagen and tissue factor become exposed to the flowing blood, thereby initiating the formation of thrombus. Endothelium

is also an important target for tumor necrosis factor (TNF) and interleukin-1 (IL-1). The endothelium synthesizes and releases platelet activating factor (PAF) in response to TNF. This activity of TNF overlaps that of IL-1, which also induces PAF production in endothelium [22]. These vessel wall alterations result in a change of endothelium from antithrombotic to thrombotic. The disrupted endothelium is the first reaction in platelet adhesion to the vessel subendothelium under physiologic blood flow [21]. In liver tissues injured by inflammation, platelets adhere to endothelial cells of sinusoids in the same way as to vessel walls [17]. A model of hepatitis, Kupffer cells produce the majority of TNF-α [23]. Under lipopolysaccharide administration in mice, TNF or IL-1 induces platelets to accumulate in the liver sinusoidal space within a few minutes by a different mechanism of aggregation [18–20].

In this study, the liver tissues of cirrhotic patients with high serum ALT level showed a significantly higher degree of inflammation than those of patients with low serum ALT level. We confirmed that, in patients with liver cirrhosis, the platelet area of the liver tissues was positively correlated with the degree of histological hepatic inflammation and negatively correlated with blood platelet count 3 months after splenectomy. In liver cirrhosis, chronic hepatic necroinflammation contributes to the accumulation of platelets in liver. We considered that patients with high serum ALT level had larger amount of platelets in liver than patients with low serum ALT level; as a result, they tended to only slightly improve thrombocytopenia after splenectomy. The mechanisms leading to thrombocytopenia with liver cirrhosis are most likely multifactorial processes [1–7]. The accumulation of platelets in the liver with chronic hepatitis and cirrhosis may be one of the important contributing factors to the therapeutic efficacy of splenectomy for thrombocytopenia.

In addition, we found megakaryocytes in the splenic tissues of most cirrhotic patients. This study also demonstrated that, in cirrhotic patients, blood platelet count and white blood cell count were higher after splenectomy than preoperative data. We considered that splenic megakaryocytes could not play major roles in platelet recovery in thrombocytopenia caused by hypersplenism with liver cirrhosis. Further biological studies should be undertaken to clarify the mechanisms and functions of megakaryopoiesis in the spleen.

In this study, in cirrhotic patients, serum total bilirubin level was lower after splenectomy compared with preoperative data. Bilirubinemia secondary to hypersplenism is caused by an increase in bilirubin production, which overloads the capacity of the liver to metabolize bilirubin [24]. To date, several reports have shown that a splenectomy accelerated hepatic regeneration and inhibits the formation of hepatic fibrosis [25–28]. Splenectomy may contribute to the decrease in total bilirubin level, but it is difficult to demonstrate any direct contribution, and care to protect liver function after operation could well have some influence.

In conclusion, in patients with liver cirrhosis, hepatic necroinflammation contributes to the accumulation of platelets in liver; therefore, in patients with high serum ALT level, improvement of thrombocytopenia by the elimination of hypersplenism was limited. Moreover, our results suggest that, in cirrhotic patients with thrombocytopenia caused by hypersplenism, serum ALT level may be a useful surrogate marker to predict the outcome of splenectomy. Additional large size and long-term studies should be undertaken to clarify this suggestion.

Acknowledgments This study was partially supported by a Health and Labor Sciences Research Grant from the Ministry of Health, Labor and Welfare Japan, regarding Research on Intractable Diseases, Portal Hemodynamic Abnormalities.

Conflict of interest None declared.

References

1. Aoki Y, Hirai K, Tanikawa K. Mechanism of thrombocytopenia in liver cirrhosis: kinetics of indium-111 tropolone labelled platelets. Eur J Nucl Med. 1993;20:123–9.
2. Schmidt KG, Rasmussen JW, Bekker C, Madsen PE. Kinetics and in vivo distribution of 111-in-labelled autologous platelets in chronic hepatic disease: mechanisms of thrombocytopenia. Scand J Haematol. 1985;34:39–46.
3. Pockros PJ, Duchini A, McMillan R, Nyberg LM, McHutchison J, Viernes E. Immune thrombocytopenic purpura in patients with chronic hepatitis C virus infection. Am J Gastroenterol. 2002;97:2040–5.
4. Aster RH. Pooling of platelets in the spleen: role in the pathogenesis of "hypersplenic" thrombocytopenia. J Clin Invest. 1966; 45:645–57.
5. Peck-Radosavljevic M. Thrombocytopenia in liver disease. Can J Gastroenterol. 2000;14(Suppl D):60D–6D.
6. Giannini E, Botta F, Borro P, Malfatti F, Fumagalli A, Testa E, et al. Relationship between thrombopoietin serum levels and liver function in patients with chronic liver disease related to hepatitis C virus infection. Am J Gastroenterol. 2003;98:2516–20.
7. Kondo R, Yano H, Nakashima O, Tanikawa K, Nomura Y, Kage M. Accumulation of platelets in the liver may be an important contributory factor to thrombocytopenia and liver fibrosis in chronic hepatitis C. J Gastroenterol. 2013;48:526–34.
8. Coon WW. Splenectomy for thrombocytopenia due to secondary hypersplenism. Arch Surg. 1988;123:369–71.
9. Kercher KW, Carbonell AM, Heniford BT, Matthews BD, Cunningham DM, Reindollar RW. Laparoscopic splenectomy reverses thrombocytopenia in patients with hepatitis C cirrhosis and portal hypertension. J Gastrointest Surg. 2004;8:120–6.
10. Sangro B, Bilbao I, Herrero I, Corella C, Longo J, Beloqui O, et al. Partial splenic embolization for the treatment of hypersplenism in cirrhosis. Hepatology. 1993;18:309–14.
11. Desmet VJ, Gerber M, Hoofnagle JH, Manns M, Scheuer PJ. Classification of chronic hepatitis: diagnosis, grading and staging. Hepatology. 1994;19:1513–20.

12. Batts KP, Ludwig J. Chronic hepatitis. An update on terminology and reporting. Am J Surg Pathol. 1995;19:1409–17.
13. Duperray A, Troesch A, Berthier R, Chagnon E, Frachet P, Uzan G, et al. Biosynthesis and assembly of platelet GPIIb-IIIa in human megakaryocytes: evidence that assembly between pro-GPIIb and GPIIIa is a prerequisite for expression of the complex on the cell surface. Blood. 1989;74:1603–11.
14. Noguchi H, Hirai K, Aoki Y, Sakata K, Tanikawa K. Changes in platelet kinetics after a partial splenic arterial embolization in cirrhotic patients with hypersplenism. Hepatology. 1995;22: 1682–8.
15. Kinuya K, Matano S, Nakashima H, Taki S. Scintigraphic prediction of therapeutic outcomes of splenectomy in patients with thrombocytopenia. Ann Nucl Med. 2003;17:161–4.
16. Sata M, Yano Y, Yoshiyama Y, Ide T, Kumashiro R, Suzuki H, et al. Mechanism of thrombocytopenia induced by interferon therapy for chronic hepatitis B. J Gastroenterol. 1997;32: 206–10.
17. Miyazawa Y, Tsutsui H, Mizuhara H, Fujiwara H, Kaneda K. Involvement of intrasinusoidal hemostasis in the development of concanavalin A-induced hepatic injury in mice. Hepatology. 1998;27:497–506.
18. Nakamura M, Shibazaki M, Nitta Y, Endo Y. Translocation of platelets into Disse spaces and their entry into hepatocytes in response to lipopolysaccharides, interleukin-1 and tumour necrosis factor: the role of Kupffer cells. J Hepatol. 1998;28:991–9.
19. Itoh H, Cicala C, Douglas GJ, Page CP. Platelet accumulation induced by bacterial endotoxin in rats. Thromb Res. 1996;83:405–19.
20. Pearson JM, Schultze AE, Jean PA, Roth RA. Platelet participation in liver injury from Gram-negative bacterial lipopolysaccharide in the rat. Shock. 1995;4:178–86.
21. Furie B, Furie BC. Mechanisms of thrombus formation. N Engl J Med. 2008;359:938–49.
22. Bussolino F, Camussi G, Baglioni C. Synthesis and release of platelet-activating factor by human vascular endothelial cells treated with tumor necrosis factor or Interleukin 1α. J Biol Chem. 1988;263:11856–61.
23. Dolganiuc A, Norkina O, Kodys K, Catalano D, Bakis G, Marshall C, et al. Viral and host factors induce macrophage activation and loss of toll-like receptor tolerance in chronic HCV infection. Gastroenterology. 2007;133:1627–36.
24. Sugawara Y, Yamamoto J, Shimada K, Yamasaki S, Kosuge T, Takayama T, et al. Splenectomy in patients with hepatocellular carcinoma and hypersplenism. J Am Coll Surg. 2000;190: 446–50.
25. Akahoshi T, Hashizume M, Tanoue K, Shimabukuro R, Gotoh N, Tomikawa M, et al. Role of the spleen in liver fibrosis in rats may be mediated by transforming growth factor β-1. J Gastroenterol Hepatol. 2002;17:59–65.
26. Ueda S, Yamanoi A, Hishikawa Y, Dhar DK, Tachibana M, Nagasue N. Transforming growth factor β-1 released from the spleen exerts a growth inhibitory effect on liver regeneration in rats. Lab Invest. 2003;83:1595–603.
27. Morinaga A, Ogata T, Kage M, Kinoshita H, Aoyagi S. Comparison of liver regeneration after a splenectomy and splenic artery ligation in a dimethylnitrosamine-induced cirrhotic rat model. HPB. 2010;12:22–30.
28. Nomura Y, Kage M, Ogata T, Kondou R, Kinoshita H, Ohshima K, et al. Influence of splenectomy in patients with liver cirrhosis and hypersplenism. Hepatol Res. 2014;44: E100–9.

J Med Ultrasonics (2014) 41:209–215
DOI 10.1007/s10396-013-0487-7

CASE REPORT

Hemodynamic changes during balloon-occluded transarterial chemoembolization (B-TACE) of hepatocellular carcinoma observed by contrast-enhanced ultrasound

Katsutoshi Sugimoto · Toru Saguchi · Kazuhiro Saito · Yasuharu Imai · Fuminori Moriyasu

Received: 19 June 2013 / Accepted: 30 July 2013 / Published online: 29 August 2013

Abstract Balloon-occluded transarterial chemoembolization (B-TACE) is able to achieve denser accumulation of Lipiodol emulsion (LE) in hepatocellular carcinoma (HCC) than conventional TACE. However, to maximize the therapeutic effect of B-TACE, it is imperative to understand the hemodynamic changes that occur during arterial occlusion. We here present two patients with HCC in whom the hemodynamic changes during arterial occlusion were depicted and evaluated by contrast-enhanced ultrasound (CEUS). Arterial flow beyond the catheter tip was observed by CEUS even after balloon occlusion. In one patient, a reduction in arterial blood flow in the HCC was observed by CEUS during balloon occlusion of the target area for embolization. After B-TACE, dense LE accumulation in the HCC nodule was confirmed by flat-panel detector CT, indicating an excellent therapeutic effect. In the other patient, no changes in arterial blood flow in the HCC nodule were observed by CEUS during balloon occlusion of the target area for embolization. After B-TACE, intermediate LE accumulation in the HCC nodule was confirmed by flat-panel detector CT, indicating an incomplete therapeutic effect. The findings obtained in the two patients presented here suggest that B-TACE can be performed more effectively and reliably by monitoring blood flow using CEUS.

Keywords Hepatocellular carcinoma · Balloon-occluded transarterial chemoembolization (B-TACE) · Sonazoid · Contrast media · Ultrasound

Introduction

In our experience, balloon-occluded transarterial chemoembolization (B-TACE) is able to achieve denser accumulation of Lipiodol emulsion (LE) in hepatocellular carcinoma (HCC) than conventional TACE. Irie et al. [1] published the findings of a study to explain this phenomenon as a preliminary report and described the mechanism for this denser accumulation of LE based on measurement of the balloon-occluded arterial stump pressure (BOASP) at the embolization portion. They concluded that dense LE accumulation in the HCC nodule could be achieved by B-TACE when the BOASP was 64 mmHg or less and that BOASP measurement was useful for predicting the degree of LE accumulation (i.e., the therapeutic effect). However, they did not evaluate the actual hemodynamic changes in the HCC nodule and adjacent liver parenchyma during balloon arterial occlusion. We believe that contrast-enhanced ultrasound (CEUS) is an effective tool for such evaluation.

Electronic supplementary material The online version of this article (doi:10.1007/s10396-013-0487-7) contains supplementary material, which is available to authorized users.

K. Sugimoto (✉) · Y. Imai · F. Moriyasu
Department of Gastroenterology and Hepatology, Tokyo Medical University, 6-7-1 Nishishinjuku, Shinjuku-ku, Tokyo 160-0023, Japan
e-mail: sugimoto@tokyo-med.ac.jp

Y. Imai
e-mail: imaiy@tokyo-med.ac.jp

F. Moriyasu
e-mail: moriyasu@tokyo-med.ac.jp

T. Saguchi · K. Saito
Department of Radiology, Tokyo Medical University, Tokyo, Japan
e-mail: saguchi@tokyo-med.ac.jp

K. Saito
e-mail: saito-k@tokyo-med.ac.jp

In order to predict the therapeutic effect of B-TACE, we have developed another useful technique based on CEUS with Sonazoid (Daiichi-Sankyo, Tokyo, Japan) during balloon arterial occlusion. With this technique, it is possible to depict and evaluate the hemodynamic changes in the HCC and adjacent liver parenchyma that occur during balloon arterial occlusion. Moreover, the blood flow data obtained by CEUS permit B-TACE to be performed more effectively and reliably.

We were unable to find any reports of this technique in the recent literature; therefore, we have written this report to describe the technique and present two illustrative clinical cases.

Case reports

The various protocols including arterial injection of Sonazoid and the consent form for the study were approved by the ethics committee of our institution, and written informed consent was obtained from each patient.

Case 1

An 81-year-old woman with hepatitis C-related cirrhosis underwent US examination at a local hospital that showed a space-occupying lesion measuring 30 mm in diameter in the right lobe of the liver. The patient was referred to our institution for further workup. Triphasic CT scanning of the lesion showed arterial hypervascularity and washout in the delayed venous phase. No other lesions were observed. Based on these findings, the lesion was judged to be a solitary classical HCC measuring 30 mm in diameter. According to the Barcelona Clinic Liver Cancer (BCLC) staging system, the patient was considered to be a candidate for local ablation therapy rather than surgical resection due to impaired liver function (i.e., Child–Pugh class B). However, the lesion was located in the liver hilum and was contiguous to relatively large vessels. The patient therefore underwent combination therapy with TACE and radiofrequency (RF) ablation. B-TACE was performed first to minimize heat loss due to perfusion-mediated tissue cooling and thus increase the therapeutic effect of RF ablation.

Abdominal angiography findings

The right hepatic artery branches from the superior mesenteric artery (SMA). Digital subtraction angiography (DSA) performed via the SMA showed a hypervascular nodule in the right lobe of the liver (Fig. 1). The main feeding artery was A7. A 3F micro-balloon catheter (Attendant LP; Terumo, Tokyo, Japan) was introduced and advanced into the posterior segment of the hepatic arterial branch. DSA also showed the hypervascular nodule. However, it was difficult to advance the micro-balloon catheter further, and selective B-TACE with miriplatine [miriplatine (Dainippon Sumitomo, Osaka, Japan) 60 mg, Lipiodol (Andre Guerbet, Aulnaysous-Bois, France) 3.5 mL, and 1 mm-Gelpart (Nippon Kayaku, Tokyo, Japan)] was therefore performed at this point (in the posterior segment artery).

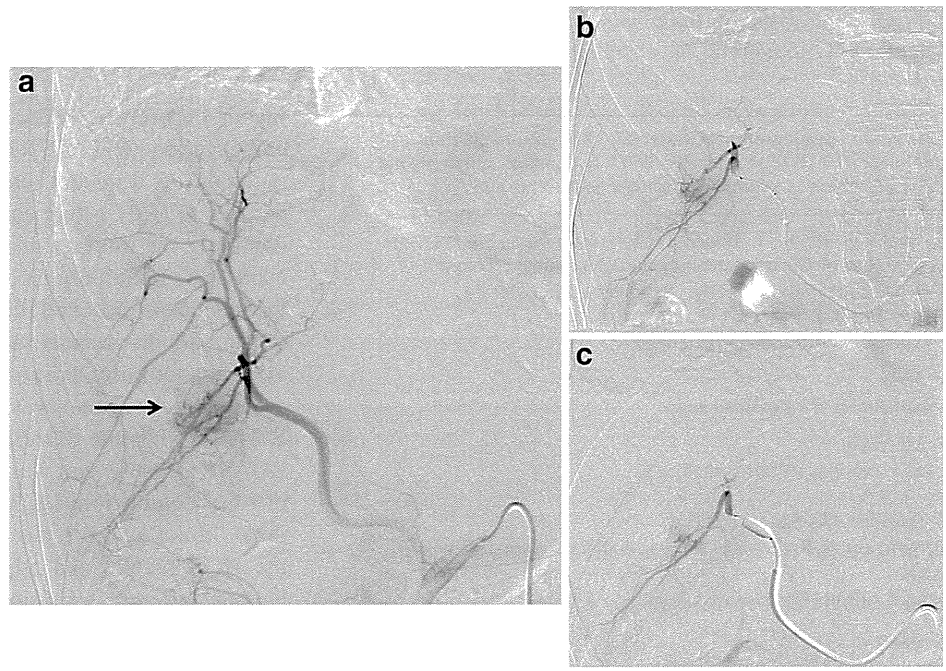

Fig. 1 **a** Case 1: 81-year-old woman with hepatitis C-related cirrhosis. Digital subtraction angiography (DSA) of the right hepatic artery via the superior mesenteric artery shows an HCC nodule (*arrow*) in segment 5. The micro-balloon catheter is placed in the posterior segment artery. DSA is performed via the posterior segment artery during balloon deflation (**b**) and inflation (**c**)

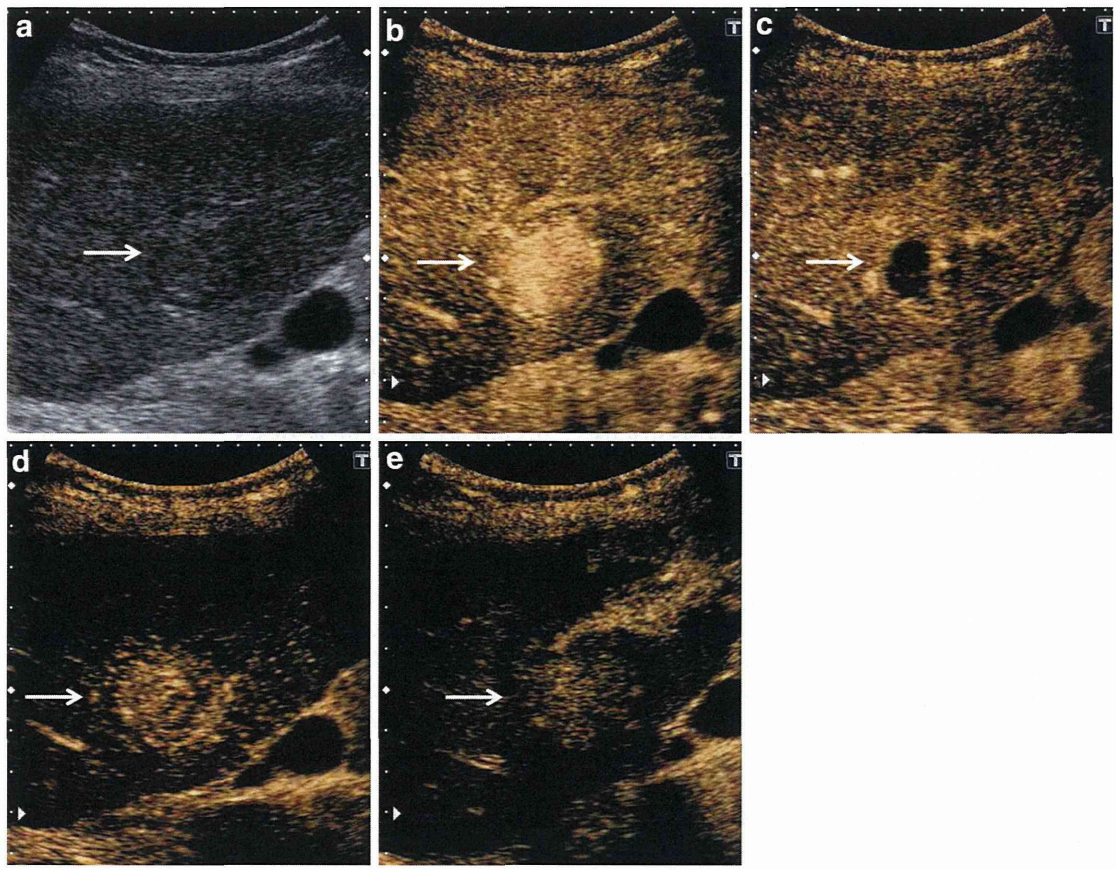

Fig. 2 Same case as in Fig. 1. The micro-balloon catheter is placed in the posterior segment artery. **a** The B-mode ultrasound (US) image shows an isoechoic HCC nodule (*arrow*). **b** Vascular phase of contrast-enhanced US (CEUS) with intravenous (IV) injection of Sonazoid during balloon deflation shows that the HCC nodule (*arrow*) is completely enhanced and that the adjacent liver parenchyma is also homogeneously enhanced. **c** Vascular phase of CEUS with IV injection of Sonazoid during balloon inflation shows that the HCC nodule (*arrow*) is partially enhanced and that the adjacent liver parenchyma is heterogeneously enhanced. **d** CEUS with intra-arterial (IA) injection of Sonazoid during balloon inflation shows that the HCC nodule (*arrow*) is slowly and completely enhanced, exhibiting sustained enhancement. On the other hand, the adjacent liver parenchyma is only slightly enhanced. **e** CEUS with IV injection of Sonazoid immediately after balloon-occluded transarterial chemoembolization (B-TACE) shows that the HCC nodule (*arrow*) is unenhanced relative to the adjacent liver parenchyma, indicating that treatment was effective

CEUS findings (micro-balloon catheter placed in the posterior segment artery)

The patient was examined by a radiologist with 10 years of experience in standard US and CEUS using a diagnostic US system (SSA-790A, Aplio XG; Toshiba Medical Systems Corporation, Tochigi, Japan) equipped with a 3.75-MHz convex transducer (PVT-375BT, Toshiba). The imaging mode employed was wideband harmonic imaging (commercially called pulse subtraction) with transmission and reception frequencies of 1.75 and 3.5 MHz, respectively. A second-generation US contrast agent, Sonazoid, was used. The contrast agent was injected intravenously as a 0.5-mL bolus into an antecubital vein via a 21-gauge peripheral intravenous cannula followed by a 10-mL saline flush or intra-arterially as a 0.05-mL bolus via a 3F micro-balloon catheter followed by a 1-mL saline flush. Dynamic scanning was then performed with the focus point set at the lower end of the lesion at a rate of 15 frames per second and with a dynamic range of 45 dB. The mechanical index was between 0.2 and 0.3 to preserve the microbubbles throughout their half-life in the microvessels and to enable real-time evaluation of the HCC nodule and parenchymal enhancement. The region of interest was observed continuously for a period of approximately 1 min from the time of injection.

- *B-mode US findings* (Fig. 2a): The image shows an isoechoic HCC nodule (arrow) in segment 6.
- *CEUS findings with intravenous (IV) injection of Sonazoid during balloon deflation* (Fig. 2b): The image shows that the HCC nodule (arrow) is completely enhanced in the arterial phase and that the adjacent liver parenchyma is also homogeneously enhanced in the portal phase.

- *CEUS findings with IV injection of Sonazoid during balloon occlusion* (Fig. 2c): The image shows that the HCC nodule (arrow) is partially enhanced in the arterial phase and that the adjacent liver parenchyma is heterogeneously enhanced in the portal phase as compared to IV injection during balloon deflation.
- *CEUS findings with intra-arterial (IA) injection of Sonazoid during balloon occlusion* (Fig. 2d): The image shows that the HCC nodule (arrow) is slowly and completely enhanced, exhibiting sustained enhancement. On the other hand, the adjacent liver parenchyma is only slightly enhanced.
- *CEUS findings with IV injection of Sonazoid immediately after B-TACE* (Fig. 2e): The image shows that the HCC nodule (arrow) is unenhanced. The adjacent liver parenchyma is also unenhanced. These findings indicate that treatment was effective.

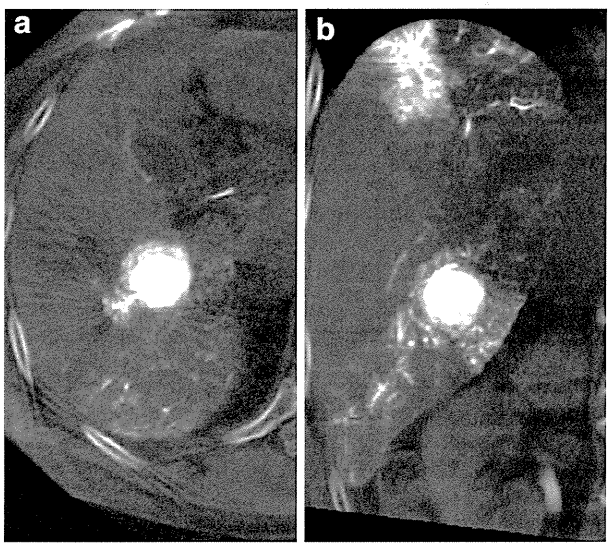

Fig. 3 Same case as in Fig. 1. Flat-panel detector CT images acquired immediately after B-TACE show dense accumulation of Lipiodol emulsion (LE) in the HCC (**a** transverse plane, **b** coronal plane)

Flat-panel detector CT findings

The images obtained immediately after B-TACE show dense accumulation of LE in the HCC nodule (Fig. 3a: transverse plane, b: coronal plane), confirming that treatment was effective.

Case 2

A 64-year-old man with multiple HCCs due to hepatitis C-related cirrhosis (Child–Pugh class A) had undergone TACE repeatedly at our institution. This time, the patient was admitted to our institution again to undergo TACE for recurrence of multiple HCCs.

Abdominal angiography findings

DSA performed via the proper hepatic artery depicted multiple hypervascular nodules in both lobes of the liver (Fig. 4). As a treatment strategy, we performed selective B-TACE for the largest nodule in the right lobe of the liver, with the other nodules treated from the right and left hepatic artery branch level. A micro-balloon catheter was advanced to A8, and DSA revealed a slightly hypervascular nodule. We anticipated that complete LE accumulation would not be achieved and that we would then perform B-TACE with miriplatine (miriplatine 50 mg, Lipiodol 2.5 mL, and 1 mm-Gelpart) at A8. The patient then received transcatheter arterial chemotherapy under balloon occlusion with miriplatine; a total of miriplatine 70 mg and Lipiodol 4.5 mL was injected from both the right and left hepatic arteries.

CEUS findings (micro-balloon catheter placed in A8)

The procedures employed for CEUS examination were the same as for case 1.

- *B-mode US findings* (Fig. 5a): The image shows a slightly hyperechoic HCC nodule in segment 8 (arrows).

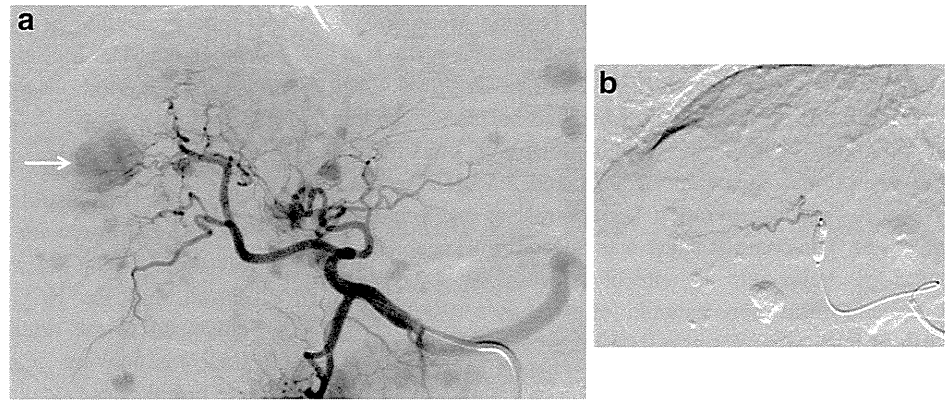

Fig. 4 Case 2: 64-year-old man with multiple HCCs in the liver. DSA performed via the proper hepatic artery shows multiple HCC nodules, with the largest HCC nodule located in segment 8 (*arrow*) (**a**). The micro-balloon catheter is placed at A8, and DSA is performed via the segment 8 artery during balloon inflation (**b**)

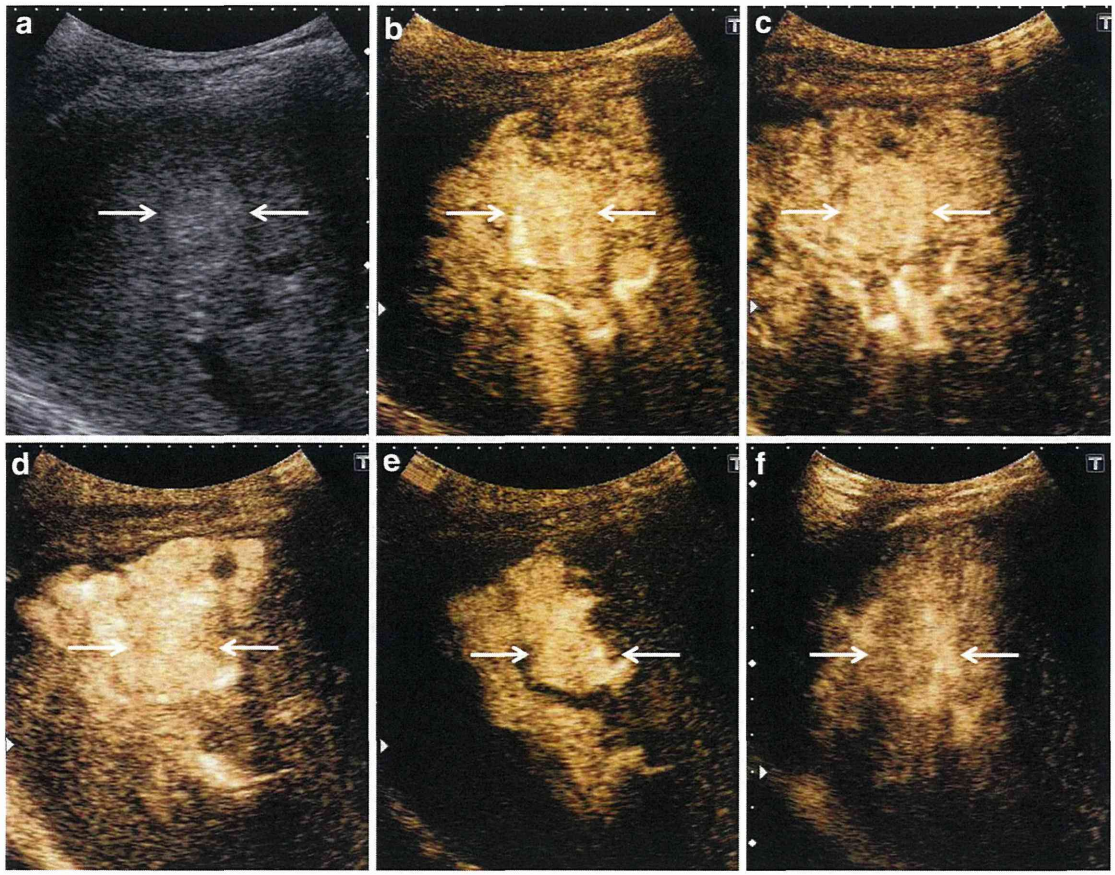

Fig. 5 Same case as in Fig. 4. The micro-balloon catheter is placed at A8. **a** B-mode US shows a slightly hyperechoic HCC nodule in segment 8 (*arrows*). **b** CEUS with IV injection of Sonazoid during balloon deflation shows that the HCC nodule (*arrows*) is completely enhanced in the arterial phase and that the adjacent liver parenchyma is also enhanced in the portal phase. **c** Vascular phase of CEUS with IV injection of Sonazoid during balloon inflation shows that the HCC nodule (*arrows*) is enhanced to the same degree as during balloon inflation in the arterial phase and that the adjacent liver parenchyma is also well enhanced in the portal phase. **d** CEUS with IA injection of Sonazoid during balloon deflation shows that the HCC nodule (*arrows*) is well enhanced and that the adjacent liver parenchyma perfused by A8 is also enhanced. **e** CEUS with IA injection of Sonazoid during balloon inflation shows that the HCC nodule (*arrows*) is slowly and strongly enhanced. On the other hand, the adjacent liver parenchyma is only partially enhanced as compared to IA injection during balloon deflation. This may be due to the obstruction of fine hepatic arteries by the micro-balloon. **f** CEUS with IV injection of Sonazoid immediately after B-TACE shows that the HCC nodule (*arrows*) is still enhanced, indicating that treatment was not effective

- *CEUS findings with IV injection of Sonazoid during balloon deflation* (Fig. 5b): The image shows that the HCC nodule (arrows) is completely and strongly enhanced in the arterial phase, followed by enhancement of the adjacent liver parenchyma.
- *CEUS findings with IV injection of Sonazoid during balloon occlusion* (Fig. 5c): The image shows that the HCC nodule (arrows) is enhanced to the same degree as during balloon deflation in the arterial phase and that the adjacent liver parenchyma is also well enhanced in the portal phase.
- *CEUS findings with IA injection of Sonazoid during balloon deflation* (Fig. 5d): The image shows that the HCC nodule (arrows) is well enhanced and that the adjacent liver parenchyma perfused by A8 is also enhanced.
- *CEUS findings with IA injection of Sonazoid during balloon occlusion* (Fig. 5e): The image shows that the HCC nodule (arrow) is slowly and completely enhanced, exhibiting sustained enhancement. On the other hand, the adjacent liver parenchyma is only partially enhanced as compared to IA injection during balloon deflation.
- *CEUS findings with IV injection of Sonazoid after B-TACE* (Fig. 5f): The image shows that the HCC nodule (arrows) is still enhanced, indicating that treatment was not effective.